Classification of Clear-Cell Sarcoma as a Subtype of Melanoma by Genomic Profiling

By Neil H. Segal, Paul Pavlidis, William S. Noble, Cristina R. Antonescu, Agnes Viale, Umadevi V. Wesley, Klaus Busam, Humilidad Gallardo, Dianne DeSantis, Murray F. Brennan, Carlos Cordon-Cardo, Jedd D. Wolchok, and Alan N. Houghton

Purpose: **To develop a genome-based classification scheme for clear-cell sarcoma (CCS), also known as melanoma of soft parts (MSP), which would have implications for diagnosis and treatment. This tumor displays characteristic features of soft tissue sarcoma (STS), including deep soft tissue primary location and a characteristic translocation, t(12;22)(q13;q12), involving *EWS* and *ATF1* genes. CCS/MSP also has typical melanoma features, including immunoreactivity for S100 and HMB45, pigmentation, *MITF-M* expression, and a propensity for regional lymph node metastases.**

Materials and Methods: **RNA samples from 21 cell lines and 60 pathologically confirmed cases of STS, melanoma, and CCS/MSP were examined using the U95A GeneChip (Affymetrix, Santa Clara, CA). Hierarchical cluster analysis, principal component analysis, and support vector machine (SVM) analysis exploited genomic correlations within the data to classify CCS/MSP.**

Results: **Unsupervised analyses demonstrated a clear distinction between STS and melanoma and, furthermore, showed that CCS/MSP cluster with the melanomas as a distinct group. A supervised SVM learning approach further validated this finding and provided a user-independent approach to diagnosis. Genes of interest that discriminate CCS/MSP included those encoding melanocyte differentiation antigens, *MITF, SOX10, ERBB3,* and *FGFR1*.**

Conclusion: **Gene expression profiles support the classification of CCS/MSP as a distinct genomic subtype of melanoma. Analysis of these gene profiles using the SVM may be an important diagnostic tool. Genomic analysis identified potential targets for the development of therapeutic strategies in the treatment of this disease.**

J Clin Oncol 21:1775-1781.

CLEAR-CELL SARCOMA (CCS), also known as melanoma of the soft parts (MSP), is an unusual malignancy of adolescents and young adults that typically arises in the deep soft tissues of the lower extremities close to tendon, fascia, and aponeuroses. CCS was originally described by Enzinger[1] in 1965 as a soft tissue sarcoma (STS). This classification was reconsidered in 1983 when Chung and Enzinger[2] changed its nomenclature to MSP. MSP was proposed to arise from a progenitor neural crest cell with the potential for melanocytic differentiation and melanin synthesis. Melanocyte progenitors normally migrate from the neural crest to the basal layer of the epidermis. In this case, the progenitor cell may not reach its final destination during embryogenesis and remains within the deeper soft tissues.

The clinical behavior of CCS/MSP demonstrates features that resemble both melanoma and STS. Like melanoma, CCS/MSP shows a propensity for regional lymph node metastasis, but it lacks a typical melanoma-like diffuse pattern of distant metastatic spread. However, this cancer resembles STS by virtue of its deep soft tissue primary location, lack of cutaneous invasion, and predilection for pulmonary metastasis.

On pathologic examination, CCSs/MSPs are positive by immunohistochemistry for melanoma markers HMB45 and S100 and contain a mixture of both stage II (unpigmented) and stage III (pigmented) melanosomes, as indicated by ultrastructural analysis.[3-6] In addition, CCSs/MSPs typically express the melanoma isoform of microphthalmia transcription factor (*MITF-M*).[4] MITF-M isoform is a transcription factor that is required for melanocytic differentiation and induces the expression of melanocyte differentiation molecules.[7-9]

Conversely, similar to a subset of STS, CCS/MSP is characterized cytogenetically by a distinct and recurrent chromosomal translocation, t(12;22)(q13;q12), in which the 5′ region of the *EWS* gene on chromosome region 22q12 recombines with the 3′ region of *ATF1* on 12q13.[10] The resulting fusion product places the carboxy terminus of *ATF1* under the constitutive regulation of the *EWS* activation domain containing repetitive sequences. The carboxy region of *ATF1* contains a functional basic leucine zipper (bZIP) DNA binding and dimerization domain. ATF1 is a transcription factor normally regulated by cyclic adenosine monophosphate (cAMP), resulting in the constitutive activation of several cAMP-inducible promoters.[11,12]

Previous studies have attempted to define CCS/MSP according to known markers of the melanocytic lineage and conventional ultrastructural and karyotypic analyses. We have applied global gene expression analysis to address the question of

From the Memorial Sloan-Kettering Cancer Center and Columbia Genome Center, Columbia University, New York, NY.

Submitted October 21, 2002; accepted January 30, 2003.

Supported in part by the Etta Weinheim Memorial Fund, New York, NY (J.D.W.); National Institutes of Health, Bethesda, MD, grant no. CA-47179 (M.F.B. and A.N.H.); Swim Across America, New York, NY; the Kennedy Family Fund, Naples, FL; and National Science Foundation, Arlington, VA, grant no. IIS-0093302 (W.S.N.).

Address reprint requests to N.H. Segal, MD, PhD, c/o Alan N. Houghton MD, Memorial Sloan-Kettering Cancer Center, 1275 York Ave, New York, NY 10021; email: segaln01@med.nyu.edu.

0732-183X/03/2109-1775/$20.00

classification. Using the Affymetrix oligonucleotide array platform (Affymetrix, Santa Clara, CA), we explored three independent bioinformatic approaches and showed that CCS/MSP represents a distinct genomic subtype of melanoma, with implications for future therapeutic strategies.

MATERIALS AND METHODS

Specimen Collection

Tissue specimens were obtained from 60 patients undergoing surgery at Memorial Sloan-Kettering Cancer Center (MSKCC, New York, NY), including four CCS/MSP, nine melanoma, and 47 STS specimens. All specimens were collected under a tissue procurement protocol reviewed and approved by the MSKCC Institutional Review Board. Representative tumor tissue was embedded in optimal cutting temperature compound and frozen as tissue blocks using liquid nitrogen. Tumor specimens were selected for analysis according to validation of histologic diagnosis.

Twenty-one cell lines were also established at MSKCC: 20 melanoma cell lines were derived from regional and distant metastases of 20 independent patients,[13] and one CCS/MSP cell line was derived in primary culture from a tumor specimen included in this study. Normal tissue RNA was obtained from Stratagene (La Jolla, CA) and Clontech (San Jose, CA). For additional details on specimens, see supplementary information at http://www.mskcc.org/genomic/ccsmsp.

Histologic and Molecular Diagnosis

In all four CCS/MSP tumor specimens and the derived cell line, histologic slides and immunostains were reviewed for confirmation of pathologic diagnosis. The presence of the *EWS-ATF1* fusion transcript was tested and confirmed in each case, as previously reported,[4] in the laboratories of Molecular Pathology at MSKCC.

Oligonucleotide Array Analysis

Cryopreserved tumor sections were homogenized under liquid nitrogen by mortar and pestle. Total RNA was extracted in Trizol reagent and purified using the Qiagen RNeasy kit (Qiagen, Valencia, CA). RNA quality was assessed by ethidium bromide agarose gel electrophoresis. Synthesis of cDNA was performed in the presence of oligo(dT)24-T7 (Genset Corp, La Jolla, CA). cRNA was prepared using biotinylated uridine triphosphate and cytosine triphosphate and hybridized to HG_U95A oligonucleotide arrays (Affymetrix). Fluorescence was measured by laser confocal scanner (Agilent, Palo Alto, CA) and converted to signal intensity by means of Microarray Suite v5.0 software (Affymetrix). For complete expression data, see supplementary information at http://www.mskcc.org/genomic/ccsmsp.

Hierarchical Cluster Analysis and Principal Component Analysis

Hierarchical cluster analysis was performed using XCluster (http://genome-www.stanford.edu/~sherlock/cluster.html), using a centered Pearson correlation coefficient distance metric and average linkage to measure cluster distances during partitioning.[14] A nonparametric bootstrap was used to estimate confidence of the cluster structure.[15] For each bootstrap sample, clustering was compared with that obtained in the original data set. Two clusters (branches of the hierarchy) were considered identical if they contained the same members. By observing the behavior of individual samples from trial to trial, additional insight could be gained into the structure of the data. That is, individual samples could be identified that contributed to the stability (or lack thereof) of particular clusters. A standard principal component analysis was performed on the full data set. Projections of the data on the principal components were visualized with XGobi (http://www.research.att.com/areas/stat/xgobi/).[16]

Support Vector Machine Analysis

The ability of a machine-learning algorithm to correctly classify each tumor type was measured using support vector machine (SVM) analysis with hold-one-out cross-validation.[17,18] In brief, during the training phase, the SVM takes as input a microarray data matrix and labels each sample as either belonging to a given class (positive) or not (negative). The SVM treats each sample in the matrix as a point in a high-dimensional feature space, where the number of genes on the microarray determines the dimensionality of the space. The SVM learning algorithm then identifies a hyperplane in this space that best separates the positive and negative training examples. The trained SVM can then be used to make predictions about a test sample's membership in the class. We used a standard hold-one-out training and testing scheme, in which the SVM is trained separately on training sets made up of all but one of the samples, and then tested on the single held-out sample. This approach allows us to collect unbiased measurements of the ability of the SVM to classify each sample. Because a classifier's performance can be hindered by the inclusion of irrelevant data, we used feature selection to identify genes that are most important for classification. The genes in the training data set were ranked in order of their proposed importance in distinguishing the positives from the negatives (as described in more detail in Gene Ranking for Feature Selection), and the top N genes were taken for each trial. The value N was varied in 12 powers of 2, ranging from 4 to 8,192. Thus the SVM was run 51 times on each of 12 different numbers of features (genes) for each of the tumor classes. Each held-out test sample was counted as either a false-positive, false-negative, true-positive, or true-negative.

Gene Ranking for Feature Selection

To select genes that were the most informative for the SVM, we tested a variety of methods, including the Fisher score method[17] and parametric and nonparametric statistics. Data reported here were derived from the Student's *t* test because it yielded the best SVM performance overall. Each gene in each training data set was subjected to the following procedure. A standard Student's *t* test was used to compare the expression in one tumor type with that in the remaining samples. The resulting *P* values were then used to rank the genes, and the desired number of genes was then selected for use. The corresponding data from the training set were used to train the SVM, and the same genes were used for the test data. It is important to note that the genes were selected solely on the basis of the training data. Finally, a statistic *t* test, as determined for all samples, was used to provide an overall ranking of the genes in order of relevance for each tumor classification. This ranking was used to provide an overview of the most important genes for distinguishing the class.

RESULTS

Cluster Analysis

We measured the gene expression profile of 81 tumor specimens and cell lines using 12,559 oligonucleotide probe sets on the U95A GeneChip. Specimens included five CCSs/MSPs (four tumor specimens and one established cell line), 29 melanomas (nine tumor specimens and 20 established cell lines), and 47 STSs (all tumor specimens). The STS specimens, which were recently examined in an independent study in tumor classification (Segal et al, manuscript submitted for publication), included leiomyosarcoma, gastrointestinal stromal tumor, synovial sarcoma, malignant fibrous histiocytoma, conventional fibrosarcoma, pleomorphic liposarcoma, dedifferentiated liposarcoma, and myxoid/round-cell liposarcoma. We explored three independent approaches to determine whether global gene expression profiling could discriminate STS from melanoma and potentially classify CCS/MSP.

We initially performed hierarchical cluster analysis to group specimens on the basis of similarity in gene expression profile. Remarkably, this analysis clearly discriminated STS and melanoma, and furthermore, it showed that CCS/MSP clustered with

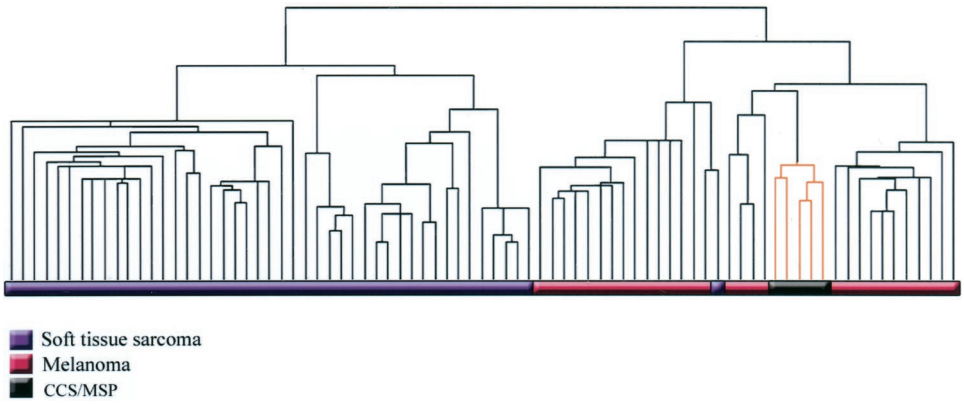

Fig 1. Hierarchical cluster analysis of 81 tumor and cell line specimens using 12,500 genes on the U95A GeneChip (Affymetrix, Santa Clara, CA). The two principal clusters correspond to melanoma and soft tissue sarcoma. Clear-cell sarcoma/melanoma of soft parts (CCS/MSP) clustered with the melanomas as a distinct group. A dedifferentiated liposarcoma clustered within the melanoma group.

the melanomas as a distinct subgroup (Fig 1). We used a bootstrap analysis to generate estimates of the robustness of the clusters. Multiple resampled data sets were generated by sampling from the data at random with replacement. This analysis revealed that some specimens were not stable. Such specimens were grouped in different trials with either the principal STS or melanoma clusters. In particular, melanoma specimens M1, M2, M5, M6, and M9 relocated 13, 49, 9, 41, and 41 times, respectively. A single dedifferentiated liposarcoma specimen, S28, clustered with the melanomas, but further histologic review of this STS specimen did not find any features to suggest melanocytic differentiation. In the same bootstrap analysis, all CCS/MSP specimens remained within the melanoma cluster in all 100 resampled data sets.

Principal Component Analysis

We applied a second unsupervised analysis to further establish the interrelationships among the samples. By visualizing projections of the data into low-dimensional spaces defined by a principal components analysis, we could observe groupings of samples reflecting underlying patterns in the expression data. The first three components, which accounted for approximately 17% variance in the data, facilitated separation of the STS and melanoma samples (Fig 2A). In agreement with the clustering results, CCS/MSP were grouped with the melanomas in this analysis. Additional component vectors accounting for an additional 12% of variability within the data were highly correlated with gastrointestinal stromal tumor, synovial sarcoma, and round-cell liposarcoma groups (data not shown). Of particular interest, component 8, accounting for approximately 2.5% of the variance, enabled separation of the CCS/MSP samples from the remaining melanoma specimens (Fig 2B).

Supervised Machine Learning Diagnosis

We applied a supervised machine-learning algorithm to the diagnosis of CCS/MSP. We trained an SVM to distinguish between melanoma and STS by the identification of a hyperplane that best discriminated these specimens. The learning efficacy of

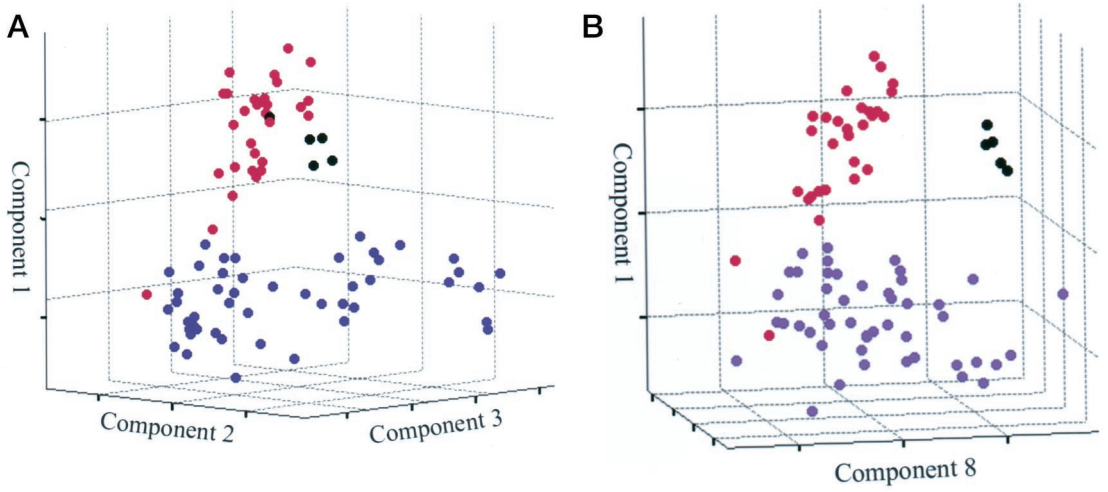

Fig 2. Relationship between melanoma (red), soft tissue sarcoma (purple), and clear-cell sarcoma/melanoma of soft parts (CCS/MSP; black) by principal component analysis. Spheres represent cases; distance between cases inversely reflects their degree of relatedness in low-dimensional space defined by principal components 1, 2, and 3 (A) or 1 and 8 (B).

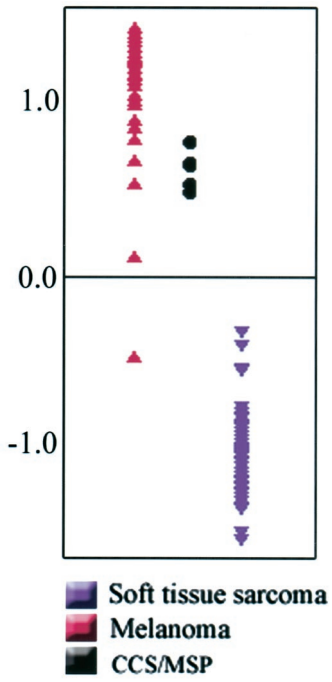

Fig 3. This one-dimensional plot of support vector machine discriminant values (left) shows each of the soft tissue sarcoma (purple) and melanoma (red) specimens during the validation stage, with a 98.5% positive predictive value. All clear-cell sarcoma (CCS)/melanoma of soft parts (MSP; black) specimens were classified as melanoma during the prediction stage.

this algorithm was demonstrated in a hold-one-out cross validation approach in which each of the 76 training specimens became unknown to the machine during both the training and predictive stages. Using 256 features (genes), SVM predicted the correct diagnosis in all STS specimens and 28 of 29 melanomas (ie, 98.5% positive predictive value). Remarkably, all CCS/MSP specimens were classified as melanomas on testing with the trained SVM (Fig 3).

Genes With Potential Biologic and Therapeutic Relevance

We used Student's *t* test analysis to identify genes for biologic discovery. The top-scoring 30 genes that discriminate CCS/MSP from STS and melanoma were cross-referenced against both the published literature and the gene ontology consortium database (http://www.geneontology.org/) using NetAffx (http://www.affymetrix.com). We discovered several genes that are implicated in diverse biologic processes, pathways, and states of differentiation (Fig 4).

Genes that discriminated CCS/MSP from STS included those implicated in cell adhesion, *CTNNA1*; cell cycle control, *CDK2*; synaptic transmission, *CNP*; transcriptional activation, *SOX10*; intracellular signaling, *STC1*; cell proliferation, *TCF8*; and the epidermal growth factor receptor, *ERBB3/HER3*.

Genes that discriminated CCS/MSP from the remaining melanoma included the cAMP-responsive element modulator, *CREM*; fibroblast growth factor receptor, *FGFR1*; and the insulin-like growth factor binding protein, *IGFBP4*.

A subset of genes, including the small monomeric GTPase *RABB33*, the proto-oncogene *MERTK*, the glycopeptide hormone *STC1*, and the neuropeptide *GAL* were shown to discriminate CCS/MSP from both STS and melanoma.

Melanoma Differentiation Antigens

We further surveyed specific genes of interest and found melanoma differentiation antigens *TYRP1*, *TYRP2/DCT*, and *MART-1* to be expressed at varying levels in the CCS/MSP specimens. *PMEL17* was most consistently expressed in all four tumors in a similar distribution to that of *MITF*. Interestingly, *SOX10*, which induces *MITF* expression,[19] was expressed in all CCS/MSP and most melanoma specimens (Fig 5).

DISCUSSION

CCS/MSP can be difficult to distinguish from malignant peripheral-nerve sheath tumors (MPNST), primary nodular cutaneous melanoma, and cutaneous melanoma metastatic to soft tissues. CCS/MSP is distinguished from MPNST by the association of the latter with nerve trunks and the presence of basal lamina around tumor cells of MPNST. Immunohistochemistry is also helpful, because amelanotic MPNST is usually negative for gp100 (encoded by *PMEL17*), whereas this melanocyte differentiation marker is usually detected in CCS/MSP. The distinction of CCS/MSP from cutaneous melanoma is more difficult, because the tumors share similar light microscopic, ultrastructural, and immunohistochemical features. If a precursor lesion, such as in situ melanoma or a nevus, is associated with a spindle-cell melanoma, the diagnosis of a primary cutaneous melanoma is straightforward. In the absence of a precursor lesion, CCS/MSP is distinguished from a primary cutaneous melanoma primarily by its anatomic location and clinical features. If a solitary melanocytic tumor is centered in deep subcutis, associated with tendinous tissue, and there is no history of a prior cutaneous melanoma, the findings favor a diagnosis of CCS/MSP. In contrast, a primary cutaneous nodular melanoma is usually a dermal-based tumor. Melanoma metastases to soft tissue derived from primary cutaneous tumors rarely occur in the absence of other evidence of metastatic disease, and the tumors tend to be more pleomorphic and mitotically active than those in CCSs/MSPs.

In samples that are difficult to diagnose, genetic studies help in making a diagnosis. Most cutaneous melanomas are markedly aneuploid[20] and frequently demonstrate diverse genetic alterations commonly involving chromosomes 1 and 5 and deletion of the 6q arm.[21,22] CCSs/MSPs are most often diploid or mildly aneuploid[20] and contain the characteristic translocation, t(12;22)(q13;q12), which involves *EWS* and *ATF1*. Confirming data in the literature show that this alteration is not found in any cases of malignant melanoma, and it is both a sensitive and a specific marker for CCS/MSP.[21] Furthermore, CCS/MSP may demonstrate unusual histology, including an alveolar growth pattern or rhabdoid cells with significant nuclear pleomorphism.[4] Despite these features being typical for STS, previous reports have shown both immunohistochemical and ultrastructural data supporting CCS/MSP as a neuroectodermal tumor with melanocytic differentiation.[3,5,23]

In this study, we show that a genomic approach to cancer classification can further clarify previously controversial diag-

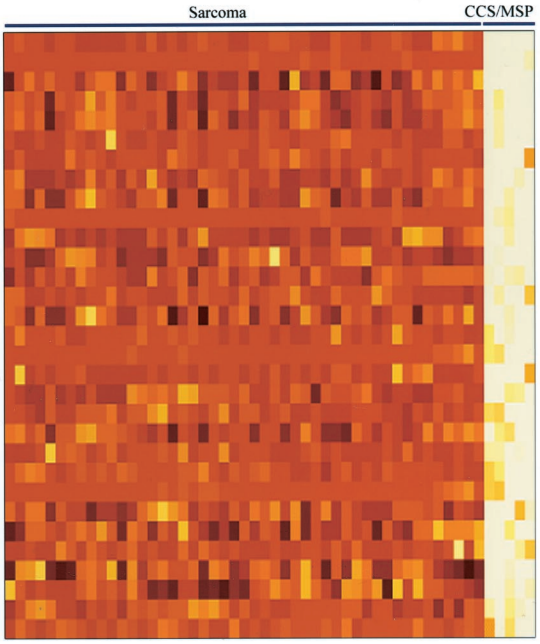

Probe set	p-value	Genbank	Symbol	Locus
32186_at	33.3	M80244	SLC7A5	16q24.3
36018_at	27.4	AJ001183	SOX10	22q13.1
344_s_at	22.6	D13146	CNP	17q21
41155_at	21.6	U03100	CTNNA1	5q31
2069_s_at	21.5	L23805	CTNNA1	5q31
34674_at	21.4	X58079	S100A1	1q21
35879_at	21	M77140	GAL	11q13.3-q13.5
33439_at	20.8	D15050	TCF8	10p11.2
41153_f_at	20.6	AF102803	CTNNA1	5q31
34922_at	19.1	AF047826	CDH19	18q22-q23
37625_at	18.9	U52682	IRF4	6p25-p23
39801_at	18.5	AF046889	PLOD3	7q22
37914_at	18.3	AB002303	ENDOFIN	5p15.2-q14.3
38121_at	18.1	X59892	WARS	14q32.31
41156_g_at	17.9	U03100	CTNNA1	5q31
235_at	17.8	M59488	S100B	21q22.3
32787_at	17.4	M34309	ERBB3	12q13
41354_at	17.4	U25997	STC1	8p21-p11.2
1201_at	17.3	D14889	RAB33A	Xq26.1
33399_at	16.4	AA142942		
2085_s_at	15.9	D14705	CTNNA1	5q31
41158_at	15.4	M54927	PHRET1	11q13.5-q14.1
1786_at	15.4	U08023	MERTK	2q14.1
1585_at	15.3	M34309	ERBB3	12q13
1792_g_at	15.2	M68520	CDK2	12q13
612_s_at	15.1	M19650	CNP	17q21
38699_at	15	X00734	TUBB5	19p13.3
32563_at	15	U51478	ATP1B3	3q22-q23
40198_at	14.6	L06132	VDAC1	5q31
41503_at	14.6	AB020661	KIAA0854	8q24.13
35086_at	14.6	AB024705	LOC51066	3p25.3

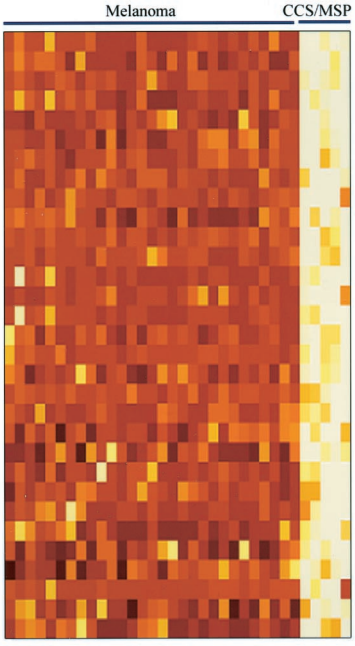

Probe set	p-value	Genbank	Symbol	Locus
1737_s_at	16	M62403	IGFBP4	17q12-q21.1
39690_at	15.4	AF002282	ALP	4q35
33439_at	14.3	D15050	TCF8	10p11.2
39781_at	14.2	U20982	IGFBP4	17q12-q21.1
32066_g_at	13.9	S68134	CREM	10p12.1-p11.1
424_s_at	13.6	X66945	FGFR1	8p11.2-p11.1
2056_at	13	M34641	FGFR1	8p11.2-p11.1
36040_at	12.6	AI337192	SH3BGR	21q22.3
35879_at	12.5	M77140	GAL	11q13.3-q13.5
41810_at	11.9	AA203545		
2057_g_at	11.9	M34641	FGFR1	8p11.2-p11.1
33442_at	11.3	AB002365	KIAA0367	9q21.31
1396_at	11.1	L27560		
41354_at	11	U25997	STC1	8p21-p11.2
38650_at	10.6	L27560		
1201_at	10.6	D14889	RAB33A	Xq26.1
41503_at	10.3	AB020661	KIAA0854	8q24.13
1202_g_at	10.1	D14889	RAB33A	Xq26.1
1786_at	10	U08023	MERTK	2q14.1
41536_at	9.79	AL022726	ID4	6p22-p21
440_at	9.68	X12492	NFIC	19p13.3
41872_at	9.5	AF073308	DFNA5	7p15
37544_at	9.44	X64318	NFIL3	9q22
33399_at	9.17	AA142942		
33316_at	9.11	AB018351	TOX	8q12.2-q12.3
38855_s_at	8.73	D82343	OLFM1	9q34.3
32065_at	8.72	S68134	CREM	10p12.1-p11.1
36168_at	8.36	X66945	FGFR1	8p11.2-p11.1
37633_s_at	8.3	J04129	PAEP	9q34
36039_s_at	8.26	X93498	SH3BGR	21q22.3
32242_at	8.05	AL038340	CRYAB	11q22.3-q23.1

Fig 4. Identification of genes for biologic discovery. Top 30 genes discriminating clear-cell sarcoma/melanoma of soft part from soft tissue sarcoma (top) and melanoma (bottom) scored by Student's *t* test analysis and sorted by increasing *P* value (shown as negative log). Light to dark color variation represents high to low levels of expression.

nostic categories. Indeed, the introduction of gene expression profile analysis calls for a revised approach in the categorization of CCS/MSP. The unsupervised analyses in this study divide malignant melanoma and STS on the basis of distinct gene expression profiles. Notwithstanding the fact that CCS/MSP is characterized by a sarcoma-like translocation, the gene expression profile of this tumor is more highly correlated with that of melanoma. This genomic classification extends beyond a handful of genetic and morphologic features to incorporate the information provided by thousands of genes. CCS/MSP specimens consistently behaved as melanomas during all bootstrapping iterations in hierarchical cluster analysis. In contrast, several melanoma specimens were observed to occasionally cluster with the STS in a subset of these analyses, using the same random genes. This observation provided support for the premise that the CCS/MSP specimens were even more melanoma-like than these melanoma specimens.

In addition, we have shown that SVM analysis predicts the precise classification of unknown specimens using data from two distinct groups, without incorporating any additional information

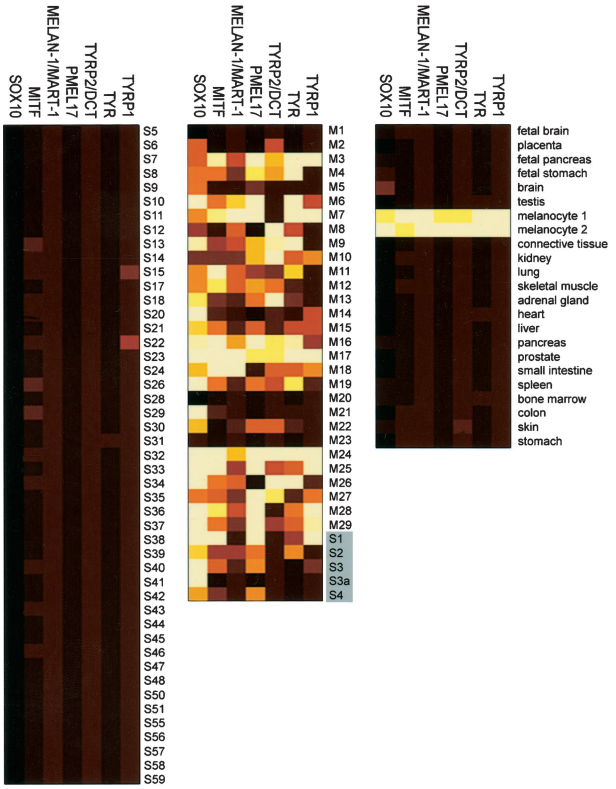

Fig 5. Expression panel of melanoma differentiation antigens as well as associated factors, MITF and SOX10, demonstrates variability in expression level in soft tissue sarcoma (left), melanoma (middle), clear-cell sarcoma/melanoma of soft parts (highlighted), and adult and fetal normal tissues (right).

from the unknown case. This method is unlike the unsupervised approaches described above, in which information from all specimens was taken into account when determining their genomic relationship and potentially influencing the outcome. The results of this diagnostic algorithm showed once more that CCS/MSP clearly belongs to the melanoma group. The observation that CCS/MSP is grouped or classified with melanoma in all analytic approaches used in this study is convincing.

It is of interest that the one melanoma that displayed the greatest tendency to cluster as an STS was a spindle-cell desmoplastic and neurotropic melanoma. Clinically, this type of melanoma often behaves similar to many sarcomas in that it is less likely to spread to lymph nodes and more likely to recur locally or metastasize to visceral sites, such as the lung, without associated nodal involvement.

One of the clearest distinctions in gene expression between CCS/MSP and STS involved genes of melanocyte differentiation. In particular, all CCS/MSP tumor specimens expressed *MITF* and *PMEL17*, whereas *MELAN-A/MART-1*, *DCT*, and *TYR* were differentially expressed in varying tumor subsets. *SOX10*, which has been reported to induce expression of *MITF*,[24] is expressed in all CCS/MSP and the majority of melanoma specimens. Another *SOX10*-inducible gene, *ERBB3/HER3*,[19] follows a similar expression pattern. Thus control of melanocytic differentiation may occur at an earlier step than previously attributed to *MITF* in this tumor type. Of interest, *SOX10* has recently been shown to be recognized by tumor-infiltrating lymphocytes in an HLA-A2–restricted fashion.[25]

FGFR1, which was shown here to be expressed in CCS/MSP, is particularly significant considering its role in angiogenesis, migration, and tumor growth. The prototype FGF family member, FGF2, is a ligand of FGFR1 and a potent mitogen in diverse cell types, including vascular endothelial cells and fibroblasts. In addition, FGF2 has been reported to act synergistically with vascular endothelial growth factor and to induce its expression (reviewed in Bikfalvi et al[26]). SU668, a potent inhibitor of tyrosine kinase activity, also inhibits FGFR, and Flk-1/kinase insert domain receptor (the vascular endothelial growth factor receptor), as well as tumor vascularization and growth of melanoma xenografts.[27] These data are support additional investigation of the effect of SU668 in the treatment of CCS/MSP.

In conclusion, gene expression profile analysis provides a unique perspective into the classification of CCS/MSP. Using three separate analytic approaches, we have shown that CCS/MSP is a distinct genomic subtype of melanoma. Our conclusion is supported by previous studies using morphologic criteria, genotypic analysis, and immunophenotypic markers.[3-6] Not only do these findings have biologic significance but they also provide practical treatment options. STSs are commonly treated with adjuvant radiation therapy, which has been shown to decrease local recurrence in a randomized trial.[28] Local radiation is rarely if ever indicated in melanoma. Furthermore, we have implicated several molecules in CCS/MSP that may be potential therapeutic targets. In particular, *pMEL17*, *TYRP2/DCT*, *MELAN-A/MART-1*, and *SOX10* could be considered for cancer vaccine strategies, and *FGFR1* could be considered as the target of the tyrosine kinase inhibitor SU6668.

ACKNOWLEDGMENT

The acknowledgment is available online at www.jco.org.

REFERENCES

1. Enzinger FM: Clear cell sarcoma of tendons and aponeuroses: An analysis of 21 cases. Cancer 18:1163-1174, 1965

2. Chung EB, Enzinger FM: Malignant melanoma of soft parts: A reassessment of clear cell sarcoma. Am J Surg Pathol 7:405-413, 1983

3. Benson JD, Kraemer BB, Mackay B: Malignant melanoma of soft parts: An ultrastructural study of four cases. Ultrastruct Pathol 8:57-70, 1985

4. Antonescu CR, Tschernyavsky SJ, Woodruff JM, et al: Molecular diagnosis of clear cell sarcoma: Detection of EWS-ATF1 and MITF-M transcripts and histopathological and ultrastructural analysis of 12 cases. J Mol Diagn 4:44-52, 2002

5. Hasegawa T, Hirose T, Kudo E, et al: Clear cell sarcoma: An immunohistochemical and ultrastructural study. Acta Pathol Jpn 39:321-327, 1989

6. Kindblom LG, Lodding P, Angervall L: Clear-cell sarcoma of tendons and aponeuroses: An immunohistochemical and electron microscopic analysis indicating neural crest origin. Virchows Arch A Pathol Anat Histopathol 401:109-128, 1983

7. Tachibana M: MITF: A stream flowing for pigment cells. Pigment Cell Res 13:230-240, 2000

8. Yasumoto K, Mahalingam H, Suzuki H, et al: Transcriptional activation of the melanocyte-specific genes by the human homolog of the mouse microphthalmia protein. J Biochem (Tokyo) 118:874-881, 1995

9. Yasumoto K, Yokoyama K, Shibata K, et al: Microphthalmia-associated transcription factor as a regulator for melanocyte-specific transcription of the human tyrosinase gene. Mol Cell Biol 14:8058-8070, 1994

10. Zucman J, Delattre O, Desmaze C, et al: EWS and ATF-1 gene fusion induced by t(12;22) translocation in malignant melanoma of soft parts. Nat Genet 4:341-345, 1993

11. Fujimura Y, Ohno T, Siddique H, et al: The EWS-ATF-1 gene involved in malignant melanoma of soft parts with t(12;22) chromosome translocation encodes a constitutive transcriptional activator. Oncogene 12:159-167, 1996

12. Brown AD, Lopez-Terrada D, Denny C, et al: Promoters containing ATF-binding sites are de-regulated in cells that express the EWS/ATF1 oncogene. Oncogene 10:1749-1756, 1995

13. Houghton AN, Real FX, Davis LJ, et al: Phenotypic heterogeneity of melanoma: Relation to the differentiation program of melanoma cells. J Exp Med 165:812-829, 1987

14. Eisen MB, Spellman PT, Brown PO, et al: Cluster analysis and display of genome-wide expression patterns. Proc Natl Acad Sci U S A 95:14863-14868, 1998

15. Felsenstein J: Confidence limits on phylogenies: An approach using the bootstrap. Evolution 39:783-791, 1985

16. Swayne DF, Cook D, Buja A: XGobi: Interactive dynamic data visualization in the X Window System. J Comput Graph Stat 7:113-130, 1998

17. Furey TS, Cristianini N, Duffy N, et al: Support vector machine classification and validation of cancer tissue samples using microarray expression data. Bioinformatics 16:906-914, 2000

18. Brown MP, Grundy WN, Lin D, et al: Knowledge-based analysis of microarray gene expression data by using support vector machines. Proc Natl Acad Sci U S A 97:262-267, 2000

19. Britsch S, Goerich DE, Riethmacher D, et al: The transcription factor Sox10 is a key regulator of peripheral glial development. Genes Dev 15:66-78, 2001

20. el-Naggar AK, Ordonez NG, Sara A, et al: Clear cell sarcomas and metastatic soft tissue melanomas: A flow cytometric comparison and prognostic implications. Cancer 67:2173-2179, 1991

21. Graadt van Roggen JF, Mooi WJ, Hogendoorn PC: Clear cell sarcoma of tendons and aponeuroses (malignant melanoma of soft parts) and cutaneous melanoma: Exploring the histogenetic relationship between these two clinicopathological entities. J Pathol 186:3-7, 1998

22. Muir PD, Gunz FW: A cytogenetic study of eight human melanoma cell lines. Pathology 11:597-606, 1979

23. Kindblom LG, Remotti HE, Aldenborg F, et al: Gastrointestinal pacemaker cell tumor (GIPACT): Gastrointestinal stromal tumors show phenotypic characteristics of the interstitial cells of Cajal. Am J Pathol 152:1259-1269, 1998

24. Watanabe KI, Takeda K, Yasumoto KI, et al: Identification of a distal enhancer for the melanocyte-specific promoter of the MITF gene. Pigment Cell Res 15:201-211, 2002

25. Khong HT, Rosenberg SA: The Waardenburg Syndrome type 4 gene, SOX10, is a novel tumor-associated antigen identified in a patient with a dramatic response to immunotherapy. Cancer Res 62:3020-3023, 2002

26. Bikfalvi A, Klein S, Pintucci G, et al: Biological roles of fibroblast growth factor-2. Endocr Rev 18:26-45, 1997

27. Laird AD, Vajkoczy P, Shawver LK, et al: SU6668 is a potent antiangiogenic and antitumor agent that induces regression of established tumors. Cancer Res 60:4152-4160, 2000

28. Pisters PW, Harrison LB, Leung DH, et al: Long-term results of a prospective randomized trial of adjuvant brachytherapy in soft tissue sarcoma. J Clin Oncol 14:859-868, 1996